

MICROSTRUCTURE AND MECHANICAL PROPERTIES OF AN AlN/Mg–Al COMPOSITE SYNTHESIZED BY Al–AlN MASTER ALLOY

Zengqiang Li, Tong Gao, Qingfei Xu, Huabing Yang, Mengxia Han, and Xiangfa Liu

Key Laboratory for Liquid-Solid Structural Evolution and Processing of Materials, Ministry of Education, Shandong University, Jinan, People's Republic of China

Copyright © 2018 American Foundry Society
<https://doi.org/10.1007/s40962-018-0261-0>

Abstract

In this work, a kind of AlN particles reinforced Mg–Al matrix composite was fabricated by introducing Al–12.5AlN master alloy into the Mg melt during casting. In the 0.8AlN/Mg–8Al composite, the nano-sized AlN particles are uniformly distributed, exhibiting a clean interface with the matrix. The introduction of AlN results in the refinement of α -Mg grains through modifying its dendrite morphology, and the β -Mg₁₇Al₁₂ intermetallic was also changed from continuous coarse-like to fine morphology.

As a result, compared with Mg–8Al matrix alloy, the tensile strength and elongation of the 0.8AlN/Mg–8Al composite were increased by 31% and 213%, respectively. The strengthening mechanism and fracture behaviors were discussed.

Keywords: Al–12.5AlN master alloy, AlN/Mg–Al composite, microstructure, mechanical properties

Introduction

It has attracted considerable attention in the development of lightweight materials in order to achieve energy saving and sustainable development in many industries, especially automotive and aerospace fields.^{1–3} Magnesium (Mg) is the lightest structural metal, with a density that is 23% of steel and 66% of aluminum; therefore it has tremendous potential to be widely used.^{4,5} However, Mg alloys generally exhibit low strength, poor ductility and lack of high-temperature creep resistance, which severely limits its applications. In order to overcome these disadvantages, different forms of reinforcements have been used to fabricate Mg-matrix composites.^{6,7} Compared with continuous fiber reinforced composites, particle reinforced Mg-matrix composites are favored by researchers due to the advantages of a relatively simple process, less expensive and isotropic properties.⁸

Recently, ceramic particles such as SiC,⁹ TiC,¹⁰ TiB₂¹¹ have been extensively used to fabricate Mg-matrix composites. Similar to Mg, AlN also exhibits a hexagonal structure and has similar lattice parameters. It has excellent properties such as a relatively low density of 3.26 g/cm³, high elastic modulus (308–315 GPa), low coefficient of

thermal expansion ($4.4 \times 10^{-6} \text{ K}^{-1}$, 293–673 K) and high thermal conductivity ($110\text{--}170 \text{ W m}^{-1} \text{ K}^{-1}$).^{12–14} Therefore, AlN may be a promising candidate using as reinforcement for producing Mg-matrix composites, which has indeed been investigated by scholars. A common method is directly introducing AlN particles into Mg melt. For instance, Cao et al.¹⁵ tried to synthesize 1 wt% AlN/AZ91D composite by directly introducing AlN powders into Mg melt followed with continuously stirring. Chen et al.¹⁶ prepared AlN reinforced Mg–9Al composites through powder metallurgy method. However, it is widely known that due to the poor wettability between ex-situ particles and Mg melt, the preparation of these composites is either hard to achieve or has unclean AlN/Mg interface. Besides, the ex-situ fine particles are also preferred to aggregate, which is detrimental to properties of the composites.^{17,18}

In order to overcome the above shortages, other methods have also been investigated. Bedolla et al.¹⁹ prepared AlN/AZ91E composite by pressureless infiltration, which performs quite attractive mechanical and thermoelectric properties due to the good wettability and capillarity between the AlN particles and Mg matrix. Yang et al.²⁰ synthesized AlN particles reinforced Mg–9Al matrix

composites through nitrogen gas bubbling method, i.e., by carrying out the reaction between N_2 and dissolved Al in the Mg melt. Even though these methods can obtain a clean reinforcement/matrix interface and is beneficial to improve the aggregation of AlN particles, they still require a complex procedure and equipment.

Using particles-contained master alloy to prepare composites may be another acceptable method, which is not only simple but also easy to conduct. For instance, the application of Al-SiC and Al-Al₃BC master alloy can easily introduce SiC and Al₃BC particles into melts.^{21,22} Therefore, in this paper, an Al-12.5AlN master alloy was used to prepare a 0.8AlN/Mg-8Al composite during casting. The stability and distribution of AlN particles and their effect on the microstructure of the composites were investigated. The tensile properties were tested, and the strengthening mechanisms were discussed.

Experimental

The raw materials in this paper contain commercial Mg ingots (99.8%, all compositions quoted in this paper are in wt% unless otherwise stated), commercial Al ingots

(99.7%) and Al-12.5AlN master alloys. High-purity Ar gas (99.9%) was selected as inert atmosphere during casting. The Al-12.5AlN master alloy is provided by Shandong Al & Mg Melt Technology Co. Ltd., which is prepared by following methods. Firstly, Al powders (99.7%, 75 μ m) and nitride plastid powders (a ball-milled mixed powder containing AlN and Al with less than 0.1 wt% of graphene) were well mixed and cold-compacted into cylindrical specimens. Then, by conducting a liquid-solid reaction at 750 °C in a vacuum electric resistance furnace, the Al-12.5AlN master alloy can be successfully fabricated. Finally, the specimens were extruded into rods at 500 °C with an extrusion ratio of 20:1.

The AlN/Mg-Al composite was prepared through the following procedures. First, Mg melt was held at 740 °C under the protection of Ar gas in a corundum crucible using a resistance furnace. Then, the preheated Al-12.5AlN master alloy was added into Mg melt, as shown in Figure 1a. The melt was then held for 20 min, during which regular stirring was applied using a four blade (pitch 45°) stainless steel impeller at 300 r/min for 30 s every 5 min. Finally, after refining and slag removal, the melt was poured into a tensile specimen steel mold preheated to

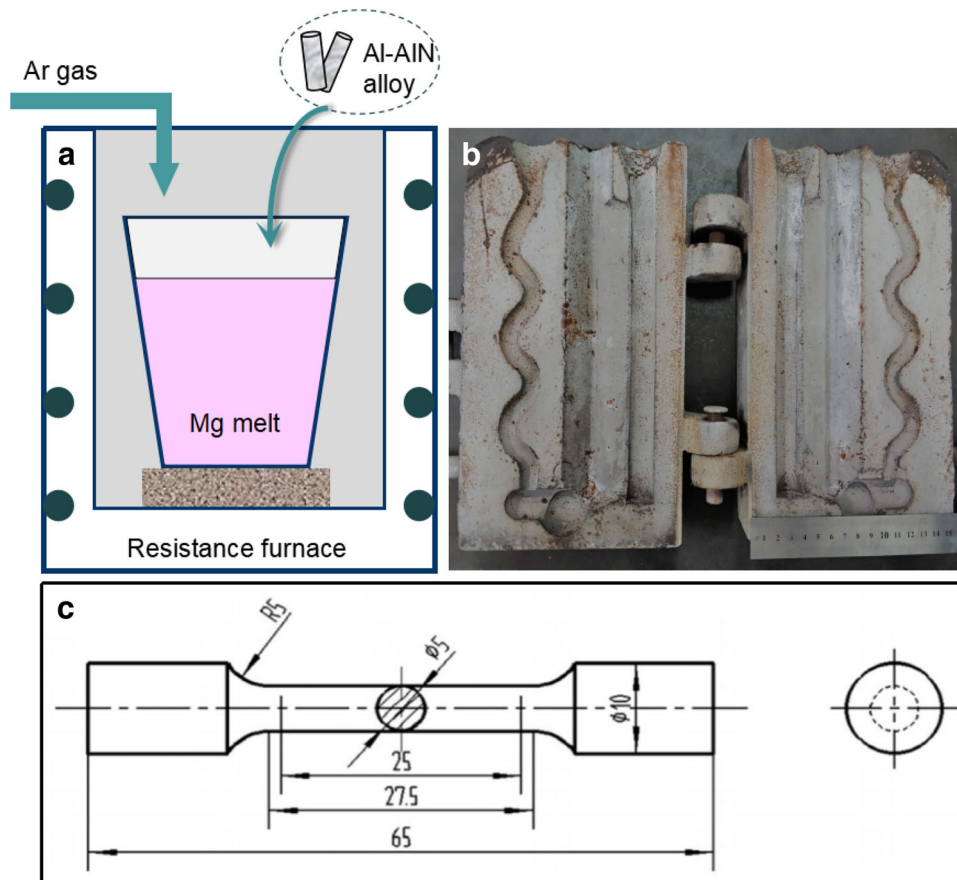


Figure 1. Experimental setup for synthesizing 0.8AlN/Mg-8Al composite (a). The schematics of tensile specimen steel mold (b) and the dog-bone-shaped specimen (c) according to ASTM standard.

200 °C, which is presented in Figure 1b. As a comparison, the Mg–8Al matrix alloy was also prepared through similar procedure.

After the samples were ground with sandpapers and polished using a MgO suspension following standard routines. A compositional analysis was performed using an X-ray fluorescence spectrometer (XRF), and the results are listed in Table 1. For microstructure analysis, as-cast and T4 (solid solution treated at 413 °C for 12 h, and then cooled in 60 °C warm water)-treated samples were prepared. Preliminary observations of the microstructure were carried out under a Leica DM2700 High-Scope Video Microscope (HSVM). Further microscopic observations were performed using field emission scanning electron microscopy (FESEM) and transmission electron microscopy (TEM) equipped with an energy-dispersive spectroscopy (EDS) detector. Phase identification of the composites was conducted by X-ray diffraction (XRD) with Cu K α radiation at 40 kV, 100 mA.

After the samples were machined to ‘dog-bone’-shaped specimen (Figure 1c) with 25 mm gauge length in compliance with ASTM E8M-16a standard, tensile properties of the 0.8AlN/Mg–8Al composite and Mg–8Al matrix alloy were tested on a WDW-100D electronic universal testing machine at room temperature. The tensile rate was set as 2.0 mm/min. Real-time monitoring of loads, stresses

and strains during testing through computer-controlled data acquisition system was obtained. The average data were acquired from at least five tensile specimens in each case.

Results and discussion

Figure 2a shows physical photograph of the Al–12.5AlN master alloy, and the corresponding microstructure is shown in Figure 2b. The size and morphology of the particles are presented in Figure 2c. It can be seen that the AlN particles are in nanometric size, with less than 200 nm in diameter.

The microstructure of the 0.8AlN/Mg–8Al composite is presented in Figure 3a. It can be observed that the AlN nanoparticles distribute relatively uniform in the matrix. Figure 3b shows corresponding XRD pattern of the composite, in which the main phases contain β -Mg₁₇Al₁₂ (Cubic, *I-43 m*, PDF# 01-1128) and AlN (Hexagonal, *P63mc*, PDF# 25-1133), except for Mg matrix. No obvious oxides (MgO, Al₂O₃ and MgAl₂O₄) or impurity phase peaks in the XRD pattern may indicate the stability and feasibility of the preparation process.

In order to highlight the influence of AlN on the microstructure of Mg–Al matrix alloy, the SEM micrographs of as-cast Mg–8Al and 0.8AlN/Mg–8Al composites are shown in Figure 4a, b. Except for α -Mg phase, the formed intermetallic is β -Mg₁₇Al₁₂, which is precipitated through a divorced eutectic reaction, thus distributing along the grain boundaries. Compared with as-cast Mg–8Al alloy, the grain size of α -Mg in the composite is decreased from 132.7 to 96.2 μ m, which is due to the refining performance of AlN particles. Besides, as can be obviously seen in Figure 4b, the secondary dendrite of α -Mg is eliminated, which may also indicate the positive effect of AlN nanoparticles. Figure 4c, d is microstructures of the T4-treated samples. In the Mg–8Al alloy, the β -Mg₁₇Al₁₂

Table 1. Chemical Composition of Mg–8Al Matrix Alloy and the 0.8AlN/Mg–8Al Composite (wt%)

Alloy	Element					
	Al	Mn	Zn	Fe	Other	Mg
Mg–8Al	7.9	< 0.001	< 0.001	< 0.002	–	Bal.
0.8AlN/ Mg–8Al	8.5	0.004	< 0.001	0.011	0.28	Bal.

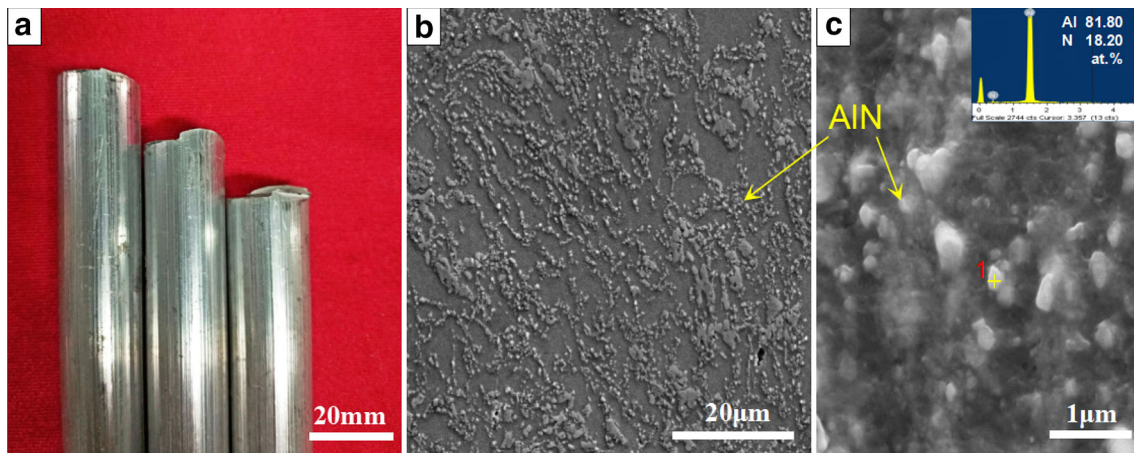


Figure 2. (a, b) The Al–12.5AlN master alloy and its microstructure; (c) morphology of AlN nanoparticles.

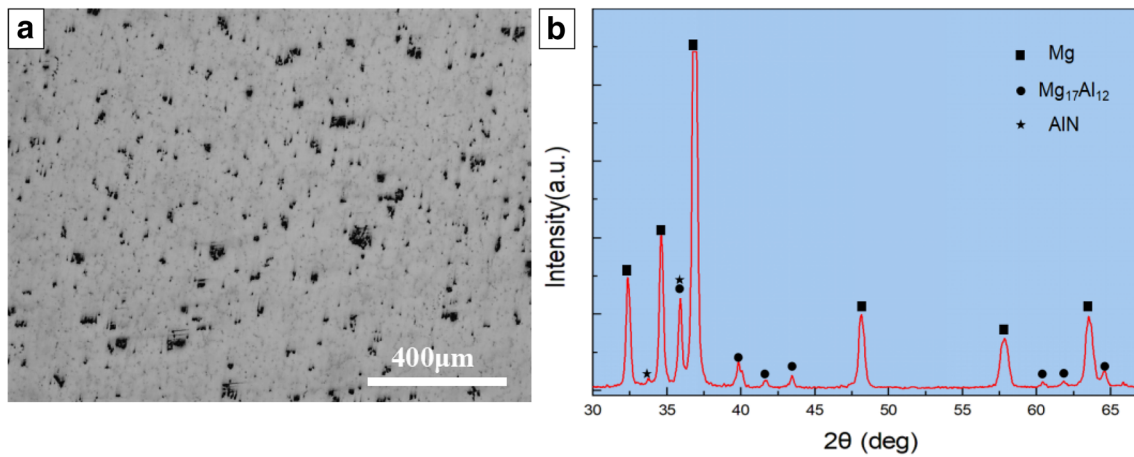


Figure 3. Microstructure (a) and XRD pattern (b) of the 0.8AlN/Mg-8Al composite.

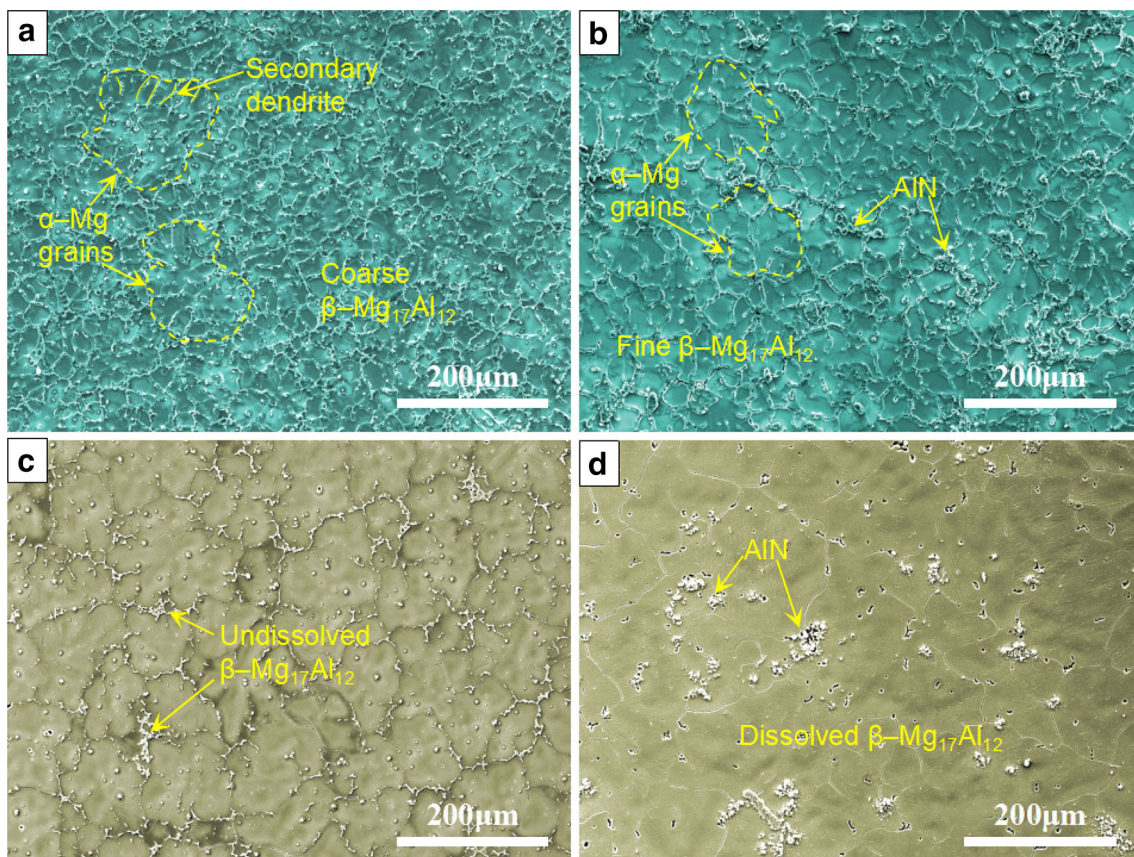


Figure 4. The microstructures of Mg-8Al matrix alloy and 0.8AlN/Mg-8Al composite: (a, b) as-cast Mg-8Al and 0.8AlN/Mg-8Al; (c, d) T4 treated Mg-8Al and 0.8AlN/Mg-8Al.

intermetallic fails to be completely dissolved during T4 treating process, and some coarse particles are left along the grain boundaries. However, in the 0.8AlN/Mg-8Al composite, no β -Mg₁₇Al₁₂ particles were obviously observed as shown in Figure 4d.

Figure 5a clearly shows the distribution of AlN particles in the composite, i.e., some AlN particles locate along the grain boundaries, while some clusters exist inside the

grains. Figure 5b shows magnified micrograph of a small cluster of particles. Based on the EDS spectrum and elemental content, the nano-sized particles were deduced to be AlN particles. Therefore, no obvious size or morphological change of AlN was detected, indicating that the AlN particles keep stable after they were introduced into the Mg-Al melt by Al-12.5AlN master alloy. To further confirm the ratiocination, TEM analysis of the 0.8AlN/Mg-8Al composite was conducted, as shown in Figure 6. From

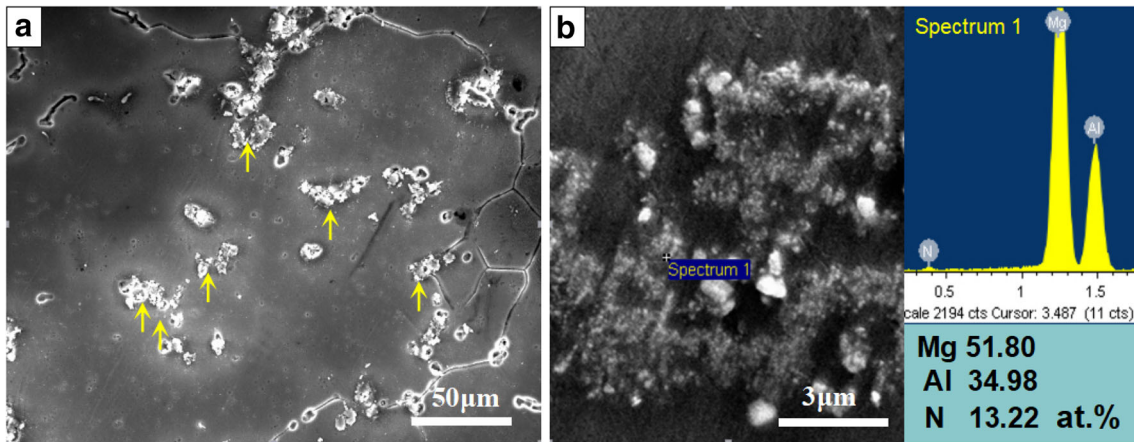


Figure 5. The distribution (a) and EDS spectrum (b) of AlN particles in the 0.8AlN/Mg-8Al composite.

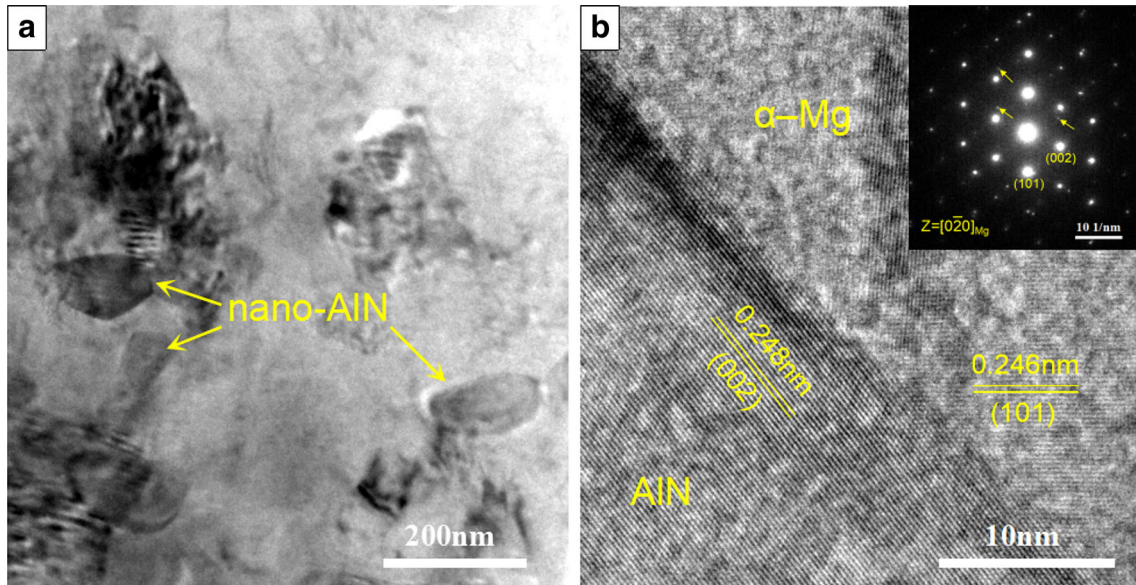


Figure 6. (a) TEM image of AlN nanoparticles in the 0.8AlN/Mg-8Al composite. (b) HRTEM image of interface between AlN and Mg matrix, and the corresponding SAED pattern.

Figure 6a, it was observed that the AlN particles are about 150 nm, again confirming its stability in Mg melt. Figure 6b shows HRTEM image of the interface between AlN and α -Mg matrix, and the corresponding selected area electron diffraction (SAED) pattern recorded near the zone axis of $[0-20]_{\text{Mg}}$ is also presented. Based on the interplanar spacing value and SAED pattern, the (002) plane of AlN was labeled (Figure 6b). What's more, the interface between AlN and Mg matrix is clean and clear.

The tensile properties at room temperature of as-cast and T4-treated Mg-8Al alloy and 0.8AlN/Mg-8Al composite were tested, and the results are listed in Table 2. It was found that the introduction of AlN nanoparticles in the Mg-8Al alloy can obviously improve the ultimate tensile strength (UTS), yield strength (YS) and elongation (δ).

Table 2. Room Temperature Tensile Properties of the Samples

Alloy	Tensile strength (MPa)	Yield strength (MPa)	Elongation (%)
As-cast Mg-8Al	133 ± 4	104 ± 2	1.5 ± 0.2
As-cast 0.8AlN/Mg-8Al	173 ± 8	106 ± 8	4.5 ± 0.3
T4 treated Mg-8Al	176 ± 5	110 ± 4	3.8 ± 0.3
T4 treated 0.8AlN/Mg-8Al	220 ± 10	123 ± 11	6.2 ± 0.3

Typical stress–strain curves of these alloys are shown in Figure 7, in which the UTS of as-cast Mg–8Al and 0.8AlN/Mg–8Al is 137 MPa and 179 MPa, while δ is 1.5% and

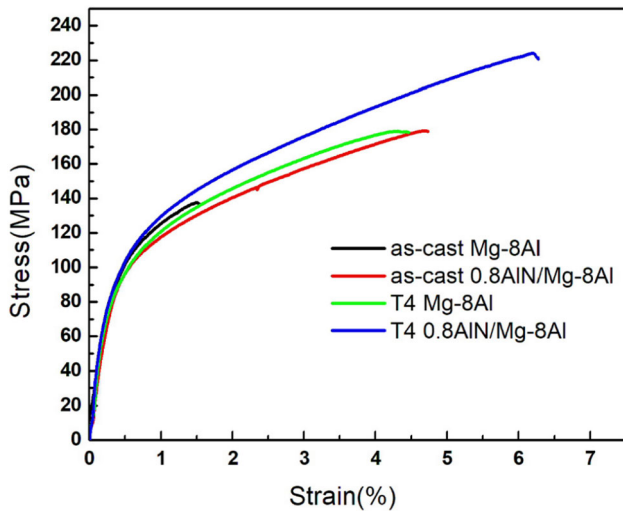


Figure 7. Typical stress–strain curves at room temperature of Mg–8Al matrix alloy and the 0.8AlN/Mg–8Al composite.

4.7%, respectively. After T4 treatment, the UTS and δ of both Mg–8Al and 0.8AlN/Mg–8Al are significantly improved when compared with the as-cast state. As expected, the 0.8AlN/Mg–8Al composite still exhibits higher UTS and δ values than the Mg–8Al matrix alloy.

The results above indicate that the 0.8AlN/Mg–8Al composite performs enhanced tensile properties, comparing with Mg–8Al matrix alloy. The mechanism can be attributed to several issues. First, since AlN has high melting point and elastic modulus, the introduction of the particles may bring attractive strengthening effect. The clean interface and good combination between distributed nanoparticles and the Mg matrix are beneficial to provide pinning effect of dislocations during tensile procedures. Secondly, the reduced grain size of α -Mg also contributes to the improvement of tensile properties, and this effect is more efficient especially in hexagonal magnesium alloys.^{20,23} Except for grain size variance, the changes in morphology and distribution of β -Mg₁₇Al₁₂ should also be a concern. Figure 8a, c shows morphology and size of the β -Mg₁₇Al₁₂ intermetallic in the Mg–8Al and 0.8AlN/Mg–8Al composites, respectively. The distribution areas of Mg matrix and β -Mg₁₇Al₁₂ are presented by different colors in Figure 8b,

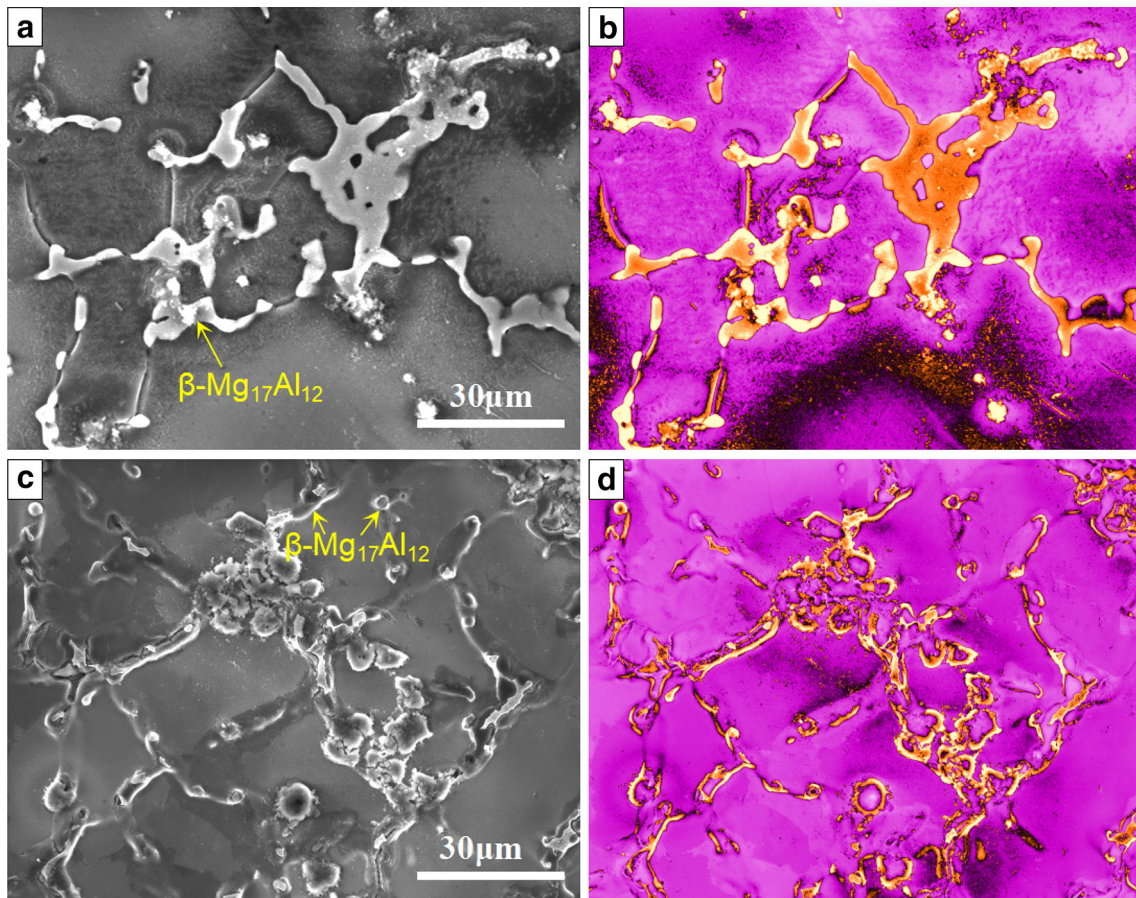


Figure 8. Micrographs of (a) β -Mg₁₇Al₁₂ phase in Mg–8Al matrix alloy; (c) β -Mg₁₇Al₁₂ phase and AlN agglomerations in 0.8AlN/Mg–8Al composite. β -Mg₁₇Al₁₂ phase is presented by yellow color, Mg matrix and AlN agglomerations are presented by pink color in (b, d), correspondingly.

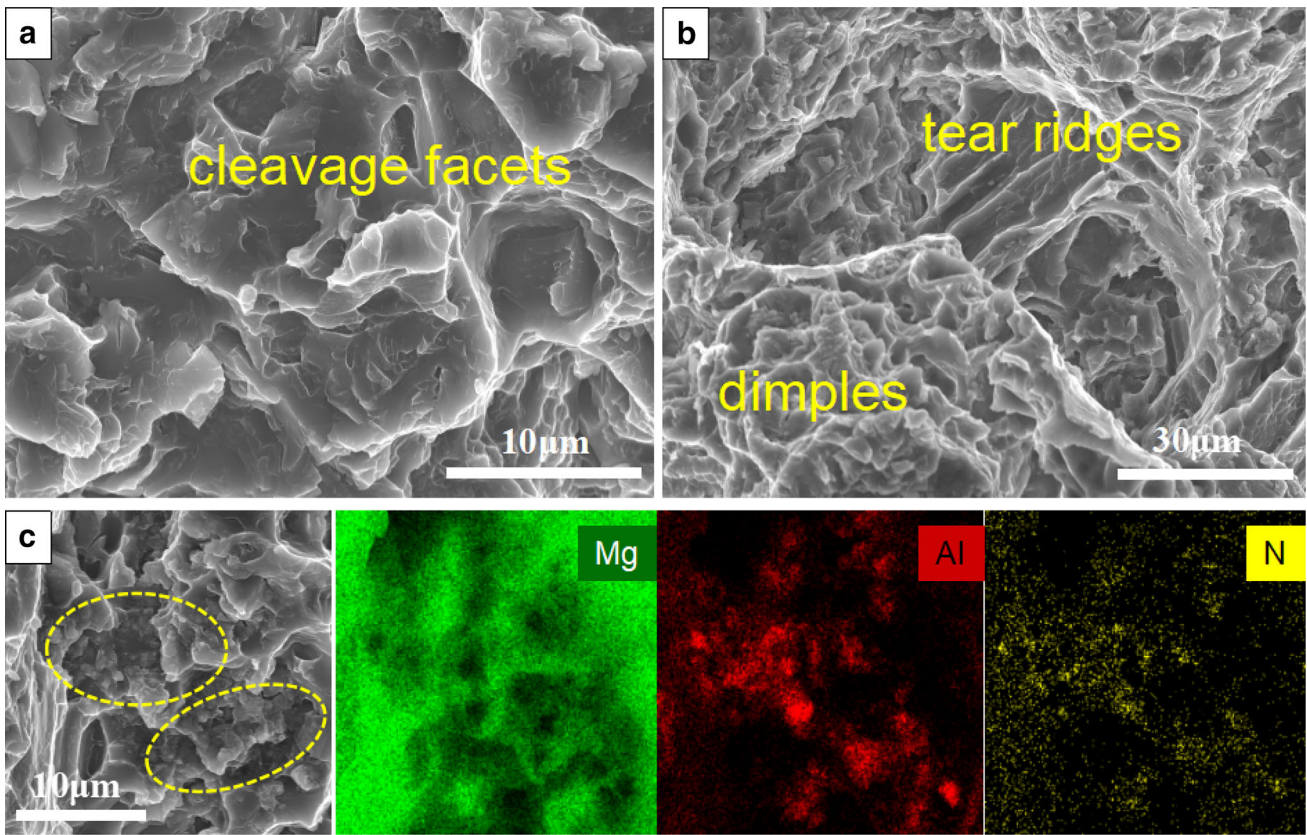


Figure 9. Micrographs of tensile fracture surface for (a) Mg-8Al matrix alloy and (b, c) 0.8AlN/Mg-8Al composite.

d. It can be found that in the Mg-8Al matrix alloy, the β -Mg₁₇Al₁₂ particles form a semi-continuous network, which is relatively coarse. However, in the 0.8AlN/Mg-8Al composite, the existence of AlN nanoparticles along grain boundaries contributes to break continuous β -Mg₁₇Al₁₂ network and change its morphology from coarse herring-bone shape to fine strip or blocky shape (Figure 8d). This variance is also confirmed by Figure 4c and d as mentioned above, which may also provide a positive effect on mechanical properties.

The micrographs of corresponding tensile fracture surface for the as-cast Mg-8Al matrix alloy and 0.8AlN/Mg-8Al composite are shown in Figure 9. It was found that the fracture surface of Mg-8Al matrix alloy consists of cleavage facets and steps (Figure 9a), i.e., the Mg-8Al matrix alloy exhibits typical brittle fracture characteristics. Due to the existence of coarse brittle intermetallic β -Mg₁₇Al₁₂ at grain boundaries, micro-cracks prefer to initiate and grow along the grains. However, in the fracture surface of 0.8AlN/Mg-8Al composite (Figure 9b), shallow dimples appear in the local area, which is the classical characteristic of ductile fracture. Besides, AlN particle clusters can be found inserted in the dimples instead of exposed on the fracture surface (Figure 9c), as shown by the scanning maps. It can be deduced that the well interfacial bonding between AlN and Mg matrix not only transfers load evenly from Mg matrix to nano-sized AlN

particles, but also avoids stress concentration. This mechanism may also be confirmed by Ref. ²⁴, which points out that the mechanical properties of particulate containing composites can be greatly improved by uniform distribution of reinforcements. Therefore, on the one hand, according to load-bearing strengthening mechanism, the matrix of the 0.8AlN/Mg-8Al composite could bear greater loads. On the other hand, the nanometric AlN particles can effectively restrict the dislocation movement in terms of Orowan strengthening mechanism.²⁵

Conclusions

In this study, 0.8AlN/Mg-8Al composite was successfully synthesized by introducing Al-12.5AlN master alloy into Mg melt through a casting method. The nano-sized (< 200 nm) AlN particles are relatively uniformly distributed in the matrix, performing good interfacial combination with the matrix. The strengthening effect of AlN and its modification performance on α -Mg grains and β -Mg₁₇Al₁₂ intermetallic contribute to the enhanced tensile properties of the composite. Compared with Mg-8Al matrix alloy, the tensile strength and elongation of the as-cast 0.8AlN/Mg-8Al composite are increased by 31% and 213%, respectively. The results in this paper may inspire new approaches for the preparation of Mg-matrix composites.

Acknowledgements

This research was financially supported by the National Natural Science Foundation of China (Nos. 51601106 and 51731007), China Postdoctoral Science Foundation (No. 2017T100489), Fundamental Research Funds of Shandong University (2016GN012).

REFERENCES

1. C. Xu, M. Zheng, S. Xu, K. Wu, E. Wang, G. Fan, S. Kamado, Improving strength and ductility of Mg–Gd–Y–Zn–Zr alloy simultaneously via extrusion, hot rolling and ageing. *Mater. Sci. Eng. A* **643**, 137–141 (2015)
2. M.K. Kulekci, Magnesium and its alloys applications in automotive industry. *Int. J. Adv. Manuf. Technol.* **39**, 851–865 (2008)
3. T. Gao, Z.Q. Li, Y.X. Zhang, J.Y. Qin, X.F. Liu, Evolution of Fe-rich phases in Mg melt and a novel method for separating Al and Fe from Al–Si–Fe alloys. *Mater. Des.* **134**, 71–80 (2017)
4. Z. Wu, W.A. Curtin, The origins of high hardening and low ductility in magnesium. *Nature* **526**, 62–67 (2015)
5. J. Hirsch, T. Al-Samman, Superior light metals by texture engineering: optimized aluminum and magnesium alloys for automotive applications. *Acta Mater.* **61**, 818–843 (2013)
6. G. Cao, H. Konishi, X. Li, Recent developments on ultrasonic cavitation based solidification processing of bulk magnesium nanocomposites. *Int. J. Metalcast.* **2**, 57–65 (2008)
7. L.G. Hou, R.Z. Wu, X.D. Wang, J.H. Zhang, M.L. Zhang, A.P. Dong, B.D. Sun, Microstructure, mechanical properties and thermal conductivity of the short carbon fiber reinforced magnesium matrix composites. *J. Alloys Compd.* **695**, 2820–2826 (2017)
8. J. Liu, C. Suryanarayana, D. Ghosh, G. Subhash, L. An, Synthesis of Mg–Al₂O₃ nanocomposites by mechanical alloying. *J. Alloys Compd.* **563**, 165–170 (2013)
9. M.J. Shen, T. Ying, F.Y. Chen, J.M. Hou, Effects of hybrid SiC_p on the microstructures and mechanical properties of AZ31B Alloy. *Int. J. Metalcast.* **11**, 266–273 (2017)
10. Q.C. Jiang, X.L. Li, H.Y. Wang, Fabrication of TiC particulate reinforced magnesium matrix composites. *Scr. Mater.* **48**, 713–717 (2003)
11. G.K. Meenashisundaram, S. Seetharaman, M. Gupta, Enhancing overall tensile and compressive response of pure Mg using nano-TiB₂ particulates. *Mater. Charact.* **94**, 178–188 (2014)
12. D. Gerlich, S.L. Dole, G.A. Slack, Elastic properties of aluminum nitride. *J. Phys. Chem. Solids* **47**, 437–441 (1986)
13. I.A. Ibrahim, F.A. Mohamed, E.J. Lavernia, Particulate reinforced metal matrix composites—a review. *J. Mater. Sci.* **26**, 1137–1156 (1991)
14. K. Komeya, H. Inoue, A. Tsuge, Role of Y₂O₃ and SiO₂ additions in sintering of AlN. *J. Am. Ceram. Soc.* **57**, 411–412 (1974)
15. G. Cao, H. Choi, J. Oportus, H. Konishi, X. Li, Study on tensile properties and microstructure of cast AZ91D/AlN nanocomposites. *Mater. Sci. Eng. A* **494**, 127–131 (2008)
16. J. Chen, C.G. Bao, W.H. Chen, L. Zhang, J.L. Liu, Mechanical properties and fracture behavior of Mg–Al/AlN composite with different particle contents. *J. Mater. Sci.* **33**, 668–674 (2017)
17. S.C. Tjong, Novel nanoparticle-reinforced metal matrix composites with enhanced mechanical properties. *Adv. Eng. Mater.* **9**, 639–652 (2007)
18. M.J. Shen, F.Y. Chen, J.M. Hou, Microstructural analysis and mechanical properties of the AZ31B matrix cast composites containing micron SiC particles. *Int. J. Metalcast.* **11**, 287–293 (2017)
19. E. Bedolla, J. Lemus-Ruiz, A. Contreras, Synthesis and characterization of Mg–AZ91/AlN composites. *Mater. Des.* **38**, 91–98 (2012)
20. C.L. Yang, B. Zhang, D.C. Zhao, H.B. Lü, T.G. Zhai, F. Liu, Microstructure and mechanical properties of AlN particles in situ reinforced Mg matrix composites. *Mater. Sci. Eng. A* **674**, 158–163 (2016)
21. X.F. Du, T. Gao, D.K. Li, Y.Y. Wu, X.F. Liu, A novel approach to synthesize SiC particles by in-situ reaction in Al–Si–C alloys. *J. Alloys Compd.* **588**, 374–377 (2014)
22. Y.F. Zhao, X. Ma, H.W. Chen, X.J. Zhao, X.F. Liu, Preferred orientation and interfacial structure in extruded nano-Al₃BC/6061 Al. *Mater. Des.* **93**, 283–290 (2016)
23. A. Azad, L. Bichler, A. Elsayed, Effect of a novel Al–SiC grain refiner on the microstructure and properties of AZ91E magnesium alloy. *Int. J. Metalcast.* **7**, 49–59 (2013)
24. M. Wang, D. Chen, Z. Chen, Y. Wu, F. Wang, N. Ma, H. Wang, Mechanical properties of in-situ TiB₂/A356 composites. *Mater. Sci. Eng. A* **590**, 246–254 (2014)
25. Q.B. Nguyen, M. Gupta, Enhancing compressive response of AZ31B magnesium alloy using alumina nanoparticles. *Compos. Sci. Technol.* **68**, 2185–2192 (2008)